Progress In Electromagnetics Research Letters, Vol. 63, 59–64, 2016

Dual-Wideband Bandpass Filter Using Open and Shorted Stubs Loaded Ring Resonator

Qian Yang[1, *], Yong-Chang Jiao[1], Zheng Zhang[1], and Nan Wang[2]

Abstract—This letter presents a dual-wideband bandpass filter (BPF) by using open and shorted stubs loaded ring resonator. The resonator can excite multiple resonant modes. The transmission zeros (TZs) analyzed by the transversal signal interference concepts can divide the resonant modes into two groups that form dual-wide passband. The even-mode resonant frequencies can be controlled by the stubs parameters, and the TZs can be tuned by the port angle independently. So the center frequency (CF) and the bandwidth of each passband can be flexibly controlled. An experimental dual-wideband BPF with CF of 1.48/5.7 GHz and 3 dB FBW of 137.8%/49.3% is implemented, and the experimental results are presented for validation.

1. INTRODUCTION

A modern high-speed data-rate wireless communication system requires wideband microwave bandpass filter (BPF) with high performances. In order to obtain wideband, multi-mode resonators (MMRs) [1–5, 7] have been extensively studied to address the requirements. These BPFs using a single resonator have the merit of compact size. A dual-band BPF using a quadruple-mode resonator with etched ground plane [1] increases the installation complexity, and the bandwidth controlled by coupling strength cannot be tuned very wide. The dual-band BPFs in [2, 3] using open stubs loaded shorted stepped-impedance resonator have multi-mode in each band to realize wideband. A penta-mode resonator is used in [4], and the BPF in [5] uses two multi-mode resonators. However, the two passbands are also not very wide. The coupled-line resonators in [6] and E-shaped resonator in [8] are used to obtain wide dual-passband. Nevertheless, the two passbands are closely spaced. Two cascading transversal filtering sections (TFSs) based on directional couplers in [7] are used to realize broadly-separated wide dual-passband. A slotted ground structure in [9] is applied to even broaden the dual passbands, while the structure is difficult to integrate.

This letter presents a novel stubs-loaded ring resonator with much wider passband than those in the reported BPFs [1–6]. By using even-odd mode analysis, the even-mode resonant frequencies can be lowered by adjusting the stubs parameters to widen the first passband. The transmission zeros (TZs) analyzed by the transversal signal interference concepts [10] can be controlled independently by the port separation angle. Both passbands center frequencies (CFs) and bandwidths can be tuned by controlling the locations of the resonant mode and TZs frequencies. Finally, a dual-wideband BPF is designed and fabricated to demonstrate the design principle. The measured results show good agreement with the simulated ones.

Received 4 August 2016, Accepted 21 September 2016, Scheduled 11 October 2016

* Corresponding author: Qian Yang (yangqianxidian@yahoo.com.cn).

[1] National Key Laboratory of Antennas and Microwave Technology, Xidian University, Xi'an 710071, P. R. China. [2] State Grid Shaanxi Electric Power Research Institute, Xi'an, Shaanxi 710100, P. R. China.

2. ANALYSIS OF THE PROPOSED RESONATOR

The geometrical schematic of the proposed resonator is shown in Figure 1(a), which is constructed by a uniform ring loaded with a shorted stub at the top point and an open stub at the bottom, whose electrical lengths are θ, θ_1, and θ_2, and characteristic impedances are Z, Z_1, and Z_2, respectively. Two $50\,\Omega$ lines are directly connected to the ring for serving as I/O ports. Its even-/odd-mode equivalent circuits are given in Figures 1(b) and (c), respectively. The resonant modes can be derived under the transverse resonant condition that the imaginary part of the two oppositely oriented input impedances at the same position is zero. The even-/odd-mode resonant conditions can be easily achieved as follows:

$$\mathrm{Im}\left(j\frac{Y_2}{2}\tan\theta_2 + \frac{Z - 2Z_1\tan\theta\tan\theta_1}{Z(j2Z_1\tan\theta_1 + jZ\tan\theta)}\right) = 0 \tag{1}$$

$$\mathrm{Im}(j\tan\theta) = 0 \tag{2}$$

The derived even-/odd-mode resonant conditions can be deduced by

$$2 - (2R_1\tan\theta_1 + \tan\theta)\tan\theta_2/R_2 - 4R_1\tan\theta\tan\theta_1 = 0 \tag{3}$$

$$\tan\theta = 0 \tag{4}$$

where R_1 and R_2 are the impedance ratios, $R_1 = Z_1/Z$, $R_2 = Z_2/Z$. The even-mode resonant frequency f_{en} can be tuned by the stubs parameters, while odd-mode resonant frequency f_{on} has no relationship with the subs. The first odd-mode resonant frequency f_{o1} occurs at the electrical length $\theta = \pi$, and $f_{on}/f_{o1} = n$ $(n = 1, 2, 3, \ldots)$.

Figure 1(d) shows the transmission line model of the proposed BPF. The angle of the port to the symmetrical plane is θ_t $(\theta_t = t\theta)$. Two different transmission paths are introduced to realize the signal transmission from Port 1 to Port 2 [10]. The $ABCD$ matrices of the transmission lines (M_{line1}-the electrical length $(1-t)\theta$ transmission line, M_{stub1}-shorted stub Z_1, M_{stub2}-open stub Z_2, M_{line2}-the electrical length $t\theta$ transmission line) are as follows:

$$M_{line1} = \begin{bmatrix} \cos(1-t)\theta & jZ\sin(1-t)\theta \\ jY\sin(1-t)\theta & \cos(1-t)\theta \end{bmatrix} \tag{5a}$$

$$M_{stub1} = \begin{bmatrix} 1 & 0 \\ -jY_1\cot\theta_1 & 1 \end{bmatrix} \tag{5b}$$

$$M_{stub2} = \begin{bmatrix} 1 & 0 \\ jY_2\tan\theta_2 & 1 \end{bmatrix} \tag{5c}$$

$$M_{line2} = \begin{bmatrix} \cos t\theta & jZ\sin t\theta \\ jY\sin t\theta & \cos t\theta \end{bmatrix} \tag{5d}$$

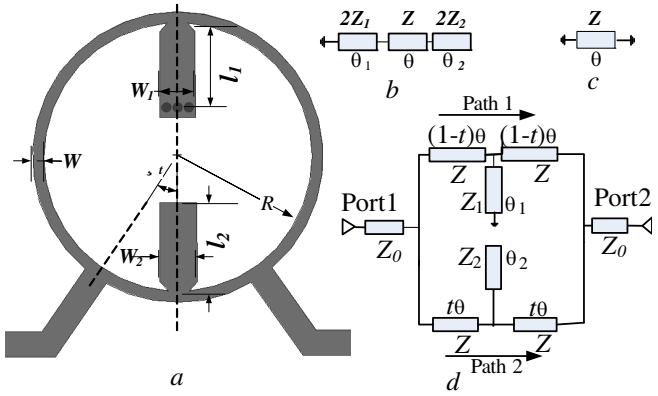

Figure 1. (a) Schematic of the proposed BPF, (b) even- and (c) odd-mode equivalent circuits, (d) transmission line model of (a).

$$\begin{bmatrix} A_1 & B_1 \\ C_1 & D_1 \end{bmatrix}_{Path_1} = M_{line1} \times M_{stub1} \times M_{line1}$$
$$= \begin{bmatrix} \cos(2(1-t)\theta) + \frac{1}{2}ZY_1 \cot\theta_1 \sin(2(1-t)\theta) & jZ\sin(2(1-t)\theta) + jZ^2Y_1\cot\theta_1\sin^2((1-t)\theta) \\ jY\sin(2(1-t)\theta) - jY_1\cot\theta_1\cos^2((1-t)\theta) & \cos(2(1-t)\theta) + \frac{1}{2}ZY_1\cot\theta_1\sin(2(1-t)\theta) \end{bmatrix} \tag{5e}$$

$$\begin{bmatrix} A_2 & B_2 \\ C_2 & D_2 \end{bmatrix}_{Path_2} = M_{line2} \times M_{stub2} \times M_{line2}$$
$$= \begin{bmatrix} \cos(2t\theta) - \frac{1}{2}ZY_2\tan\theta_2\sin(2t\theta) & jZ\sin(2t\theta) - jZ^2Y_2\tan\theta_2\sin^2(t\theta) \\ jY\sin(2t\theta) + jY_2\tan\theta_2\cos^2(t\theta) & \cos(2t\theta) - \frac{1}{2}ZY_2\tan\theta_2\sin(2t\theta) \end{bmatrix} \tag{5f}$$

After $ABCD$- and Y-parameter conversations, S-parameter of the filter can be expressed as

$$S_{21} = \frac{-Y_{21}Y_0}{(Y_0 + Y_{11})^2 - Y_{21}^2} \tag{6}$$

When $S_{21} = 0$, the transmission zeros of the circuit can be obtained from the conditions that

$$2\sin\theta\cos((1-2t)\theta) + \sin^2((1-t)\theta)\cot\theta_1/R_1 - \sin^2(t\theta)\tan\theta_2/R_2 = 0 \tag{7}$$

From Eq. (7), the TZs can be controlled by the stubs parameters and port angle ratio. When the resonator is chosen, the TZs can also be tuned by the port angle, which increases the design freedom. Equations (3), (4), and (7) can be used to determine all the frequency locations of even-/odd-mode transmission poles (TPs) and TZs. In order to observe the influence of the stubs, all TPs and TZs are normalized to the first odd-mode frequency f_{o1}, at which the electrical length $\theta = \pi$.

Figure 2 shows the variation of TPs and TZs versus designing parameters, where f_{ei}, f_{oi}, and f_{zi} ($i = 1, 2, 3, \ldots$) denote the ith resonant even mode, odd mode, and TZ frequency of the resonator, respectively. From Figures 2(a) and 2(b), it is concluded that the even-mode resonant frequencies f_{en} decrease rapidly with the increase of the electrical lengths θ_1 and θ_2. The influence of the short stub length l_1 on TPs is the same as that of the open stub length l_2. On the other hand, more TZs are produced by the increase of the stub length l_1 than the increase of the open stub length l_2, which can be seen from Figures 2(a) and 2(b). As the stubs increase, the electrical length of even-mode equivalent circuit, $f_{e1} < f_{o1}$. The electrical length ratios θ_1/θ and θ_2/θ dominate f_{en}, and as a result, we can increase the electrical length ratios to lower f_{e1} to obtain wide first passband. When the lengths ratios of the stubs are chosen to be small as 0.2, it can be seen in Figures 2(c) and 2(d) that the impedance ratios R_1 and R_2 have little influence on the TPs. The first even resonant mode frequency f_{e1} changes from $0.4f_{o1}$ to $0.26f_{o1}$ when the impedance ratio R_1 changes from 0.1 to 2. On the other hand, the first even resonant mode frequency f_{e1} changes from $0.25f_{o1}$ to $0.41f_{o1}$ when the impedance ratio R_2 changes from 0.1 to 2. The variation extent of the first even mode is relatively large while the variation of the higher even modes is small. The first three even-mode resonant frequencies f_{e1}, f_{e2}, and f_{e3} decrease with the increase of R_1 but increase with the decrease of R_2. So smaller R_1 and larger R_2 can lower f_{e1}. However, the even-mode resonant frequencies f_{e5}, f_{e6}, and f_{e7} increase as R_1 increases but decrease as R_2 decreases.

The TZs have great relationship with all the stubs parameters. The TZs decrease rapidly with the increase of stubs lengths. The variation tendency of TZs versus R_1 and R_2 is similar to that of TPs. And there exit two or three TZs between two adjacent resonant modes, which can be used to broaden the stopband. In addition, it is shown in Figure 2(e) that the TZs can be independently tuned by the port angle ratio t. The positions of TPs can determine the CF and control the FBW. The design graph can also be used to design multi-passband filters.

To design a dual-wideband BPF, it can be seen from Figure 2 that when $R_1 = R_2 = 0.5$, $\theta_1/\theta = \theta_2/\theta = 0.2$, and $t = 0.2$, the TPs f_{e1},f_{o1}, and f_{e2} form the first passband with CF at about $(f_{e1} + f_{e2})/2$. The TPs f_{e3}, f_{o2}, f_{e4}, f_{o3}, and f_{e5} build up the second passband with CF at about $(f_{e3} + f_{e5})/2$. To broaden the stopband between two passbands, the port angle ratio t is chosen to be

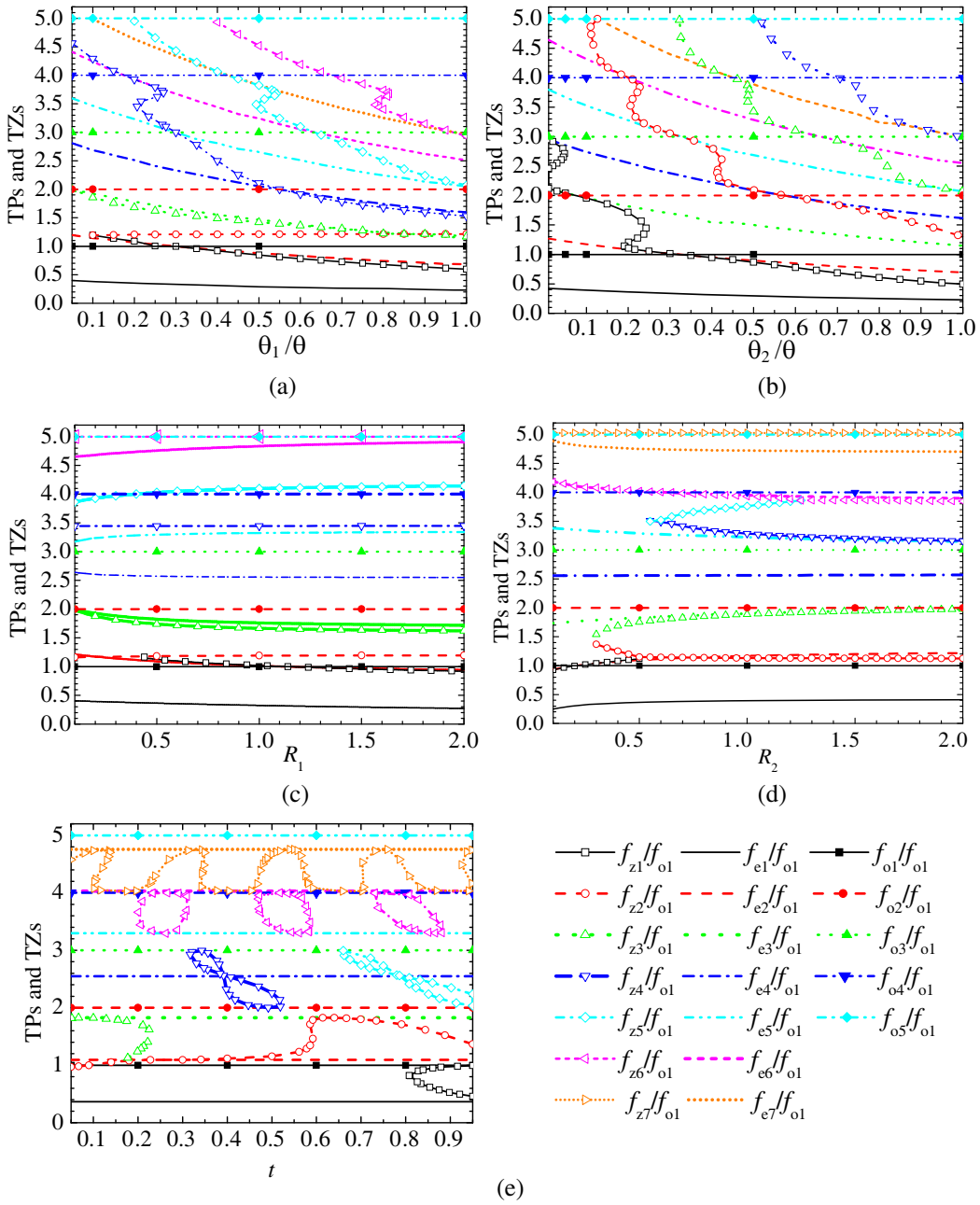

Figure 2. Variation of TPs and TZs versus varied (a) θ_1/θ, (b) θ_2/θ, (c) R_1, (d) R_2, and (e) t when one parameter changes, the remaining design parameters have fixed values of $R_1 = 0.5$, $R_2 = 0.5$, $\theta_1/\theta = 0.2$, $\theta_2/\theta = 0.2$.

0.2. There are three TZs between the two passbands and three TZs to the higher spurious passband. The return losses (RLs) of the two passbands cannot be tuned independently. They have relationship with the ring impedance Z, which is shown in Figure 3. The RL of the first passband RL1 gets higher with the increase of Z, while the RL of the second passband RL2 gets lower with the increase of Z.

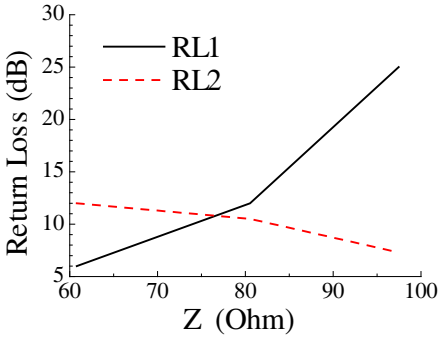

Figure 3. Variation of return losses versus varied impedance Z.

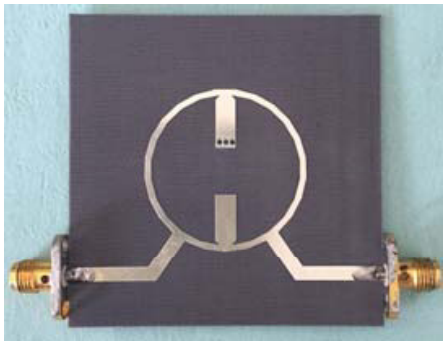

Figure 4. The photograph of the proposed filter.

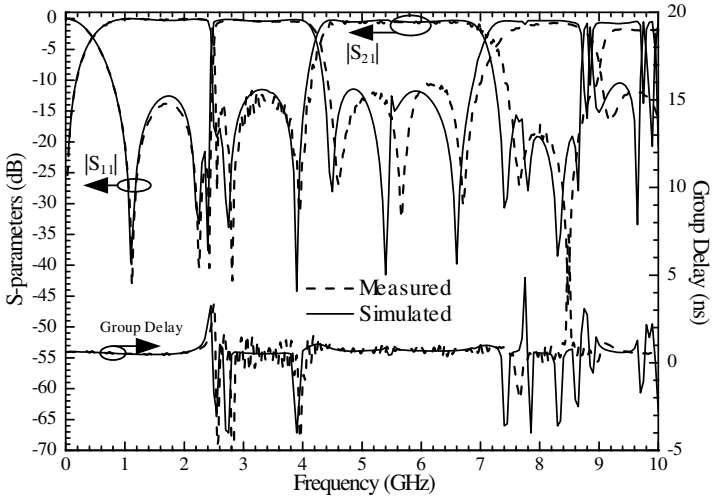

Figure 5. The simulated and measured results of the S-parameters and group delay.

3. FILTER DESIGN, FABRICATION AND MEASUREMENT

To verify the proposed design method, a dual-wideband BPF is simulated and fabricated on a substrate with relative dielectric constant of 2.65, thickness of 1 mm, and loss tangent of 0.003. For designing a dual-band BPF with the first passband CF of $f_{c1} = 1.5$ GHz, the second passband CF of $f_{c2} = 5.7$ GHz, and first passband 3 dB FBW of 135%. θ is set to be 0.6π at f_{c1}. The return losses of the two passbands should be larger than 10 dB. In order to achieve the required external quality factor and consider the impedance discontinuities, the full-wave electromagnetic simulator Ansoft HFSS is used to optimize the parameters. The optimized values of parameters are $R = 14.4$ mm, $W = 1.2$ mm, $l_1 = 8.5$ mm, $W_1 = 3.8$ mm, $l_2 = 9.4$ mm, $W_2 = 4$ mm, and $\theta_t = 35°$. The circuit size is about $0.22\lambda_g \times 0.22\lambda_g$, where λ_g is the guided wavelength at f_{c1}.

A photograph of the fabricated filter is shown in Figure 4. Figure 5 shows the simulated and measured results of the S-parameters and group delay. The measured CFs and 3 dB FBWs of the two passbands are 1.48/5.7 GHz and 137.8%/49.3%, respectively. The measured insertion losses (ILs) at the two CFs are 0.2/0.8 dB. The TPs f_{e3} and f_{e5} are close to TZs, so the second passband has three TPs f_{o2}, f_{e4}, and f_{o3}. The filter also has a sharp-skirt and flat group delay. The discrepancies between the simulated and designed results may be due to the ignored transmission line discontinuity and fabrication tolerances. Table 1 shows that the proposed dual-wideband BPF has the advantages of low IL, wide FBW, sharp skirt, and simple circuit topology. The roll-off rate (ζ_{ROR}) in Table 1 is defined as that in [1].

Table 1. Comparison with some reported wideband BPFs.

Ref.	CF (GHz)/3-dB FBW	IL at CF (dB)	ζ_{ROR} (dB/GHz)	Size ($\lambda_g \times \lambda_g$)
Filter A in [1]	1.96/57.1%, 5.58/20.8%	0.52, 1.1	63/44.7, 70.8/50	0.40×0.05
[2]	1.92/66.7%, 5.44/28.3%	0.3, 0.5	23/85, 33/27	0.213×0.134
Filter A in [3]	1.49/52.4%, 6.44/52.6%	0.1, 0.8	–	0.135×0.123
[4]	3.32/27.71%, 5.32/19.17%	0.62, 0.91	–	0.18×0.4
[5]	2.34/25.6%, 3.46/21.4%	0.84, 1.21	–	0.2×0.21
Filter I in [6]	0.9/37.9%, 1.575/36.9%	0.99, 1.32	–	0.14×0.19
This work	1.48/137.8%, 5.7/49.3%	0.2, 0.8	41.5/377.8, 59/42.5	0.22×0.22

4. CONCLUSIONS

A dual-wideband BPF using a shorted and an open stubs loaded ring resonator is proposed. The filter has an ultra-wide first passband. Besides tuning the characteristic impedance and electrical length ratios of the stubs, the port separation angle can also be tuned to adjust the transmission zero positions, making the filter obtain good passband and stopband performance. With a simple structure and good performance, the proposed filter is attractive to modern high data-rate system applications.

REFERENCES

1. Xu, J., W. Wu, and C. Miao, "Compact and sharp skirts microstrip dual-mode dual-band bandpass filter using a single quadruple-mode resonator (QMR)," *IEEE Trans. Microw. Theory Tech.*, Vol. 61, No. 3, 1104–1113, Mar. 2013.
2. Xu, J., Y.-X. Ji, C. Miao, and W. Wu, "Compact single-/dual-wideband BPF using stubs loaded SIR (SsLSIR)," *IEEE Microw. Wireless Compon. Lett.*, Vol. 23, No. 7, 338–340, Jul. 2013.
3. Xu, J., W. Wu, and C. Miao, "Compact microstrip dual-/tri-/quad-band bandpass filter using open stubs loaded shorted stepped-impedance resonator," *IEEE Trans. Microw. Theory Tech.*, Vol. 61, No. 3, 3187–3199, Sep. 2013.
4. Li, J., S.-S. Huang, and J.-Z. Zhao, "Compact dual-wideband bandpass filter using a novel penta-mode resonator (PMR)," *IEEE Microw. Wireless Compon. Lett.*, Vol. 24, No. 10, 668–670, Oct. 2014.
5. Li, J., S.-S. Huang, H. Wang, and J.-Z. Zhao, "A novel compact dual-wideband bandpass filter with multi-mode resonators," *Progress In Electromagnetics Research Letters*, Vol. 51, 79–85, 2015.
6. Kuo, J.-T., C.-Y. Fan, and S.-C. Tang, "Dual-wideband bandpass filters with extended stopband based on coupled-line and coupled three-line resonators," *Progress In Electromagnetics Research*, Vol. 124, 1–15, 2012.
7. Sánchez-Soriano, M. Á. and R. Gómez-García, "Sharp-rejection wide-band dual-band bandpass planar filters with broadly-separated passbands," *IEEE Microw. Wireless Compon. Lett.*, Vol. 25, No. 2, 97–99, Feb. 2015.
8. Wu, Y.-L., C. Liao, and X.-Z. Xiong, "A dual-wideband bandpass filters baded on E-shaped microstrip SIR with improved upper-stopband performance," *Progress In Electromagnetics Research*, Vol. 108, 141–153, 2010.
9. Wang, X.-H., B.-Z. Wang, and K. J. Chen, "Compact broadband dual-band bandpass filters using slotted ground structures," *Progress In Electromagnetics Research*, Vol. 82, 151–166, 2008.
10. Feng, W.-J., W.-Q. Che, Y.-M. Chang, S.-Y. Shi, and Q. Xue, "High selectivity fifth-order wideband bandpass filters with multiple transmission zeros based on transversal signal-interactrion concepts," *IEEE Trans. Microw. Theory Tech.*, Vol. 61, No. 1, 87–97, Jan. 2013.